한국소음진동공학회 2012년 추계학술대회논문집, pp. 630~635

Research on the Effects of Boundary Element Characteristics on Reconstruction Accuracy by BEM-based NAH

Hai-Bin Zhang[1,2]·Yang-Hann Kim[2,*]·Wei-Kang Jiang[1]

1. State Key Laboratory of Mechanical System and Vibration, Institute of Vibration, Shock and Noise, Shanghai Jiaotong University, Shanghai 200240, China.

2. Department of Mechanical Engineering, Center for Noise and Vibration Control (NOVIC), Korea Advanced Institute of Science and Technology (KAIST), Science Town, Daejeon 305-701, Korea.

Key Words : Boundary element method, Nearfield acoustic holography, Reconstruction accuracy

ABSTRACT

Nearfield acoustic holography method predicts an unmeasured sound field, therefore it depends on its prediction methods. In particular, if one has radiators or scatters, which cannot be expressed by simple geometry, then inverse boundary element method (BEM) is normally employed to reconstruct the sound field induced by sound sources with irregular profiles. The characteristics of boundary element, including the element shape, characteristic length, order of shape function and others, affect the reconstruction error. Investigating the errors by means of changing these factors will provide a guide line for selecting appropriate factors, associated with the elements of BEM. These factors are investigated by numerical simulations, and the accuracies with respect to the variant factors are compared. Novel suggestions for selecting appropriate boundary element factors are described based on the simulation results.

1. Introduction

The nearfield acoustic holography (NAH) method is a powerful tool for visualizing the sound field due to its high resolution and fine reconstruction accuracy. NAH method is calculated in different numerical ways according to the sound source profiles. The NAH method based on Fourier acoustic is computationally very efficient, but the geometries of the sound sources are limited to planar, cylindrical and spherical geometries [1-2]. The measurement points on the hologram surface are restricted as distributing with equal distance in each direction and the hologram must be conformal to the source surface. To analyze the arbitrarily shaped sources, NAH methods based on the boundary element method (BEM) [3-7] and wave superposition method [8-9] are appropriate. The latter two methods do not require the regular measurements and conformal holograms. The statistically optimized nearfield acoustic holography (SONAH) [10] reconstructs the patch sound field in a least mean square sense by the hypothesis that the sound field is the superposition of a series of elemental waves. SONAH is an effective method without the limitation on hologram shape.

The reconstruction accuracy is the most important issue in NAH procedures [2]. The reconstruction accuracy in BEM-based NAH is our main study objective in this present paper. Usually, the commonly accepted rule of thumb is to use six linear elements per wavelength for harmonic acoustics. Marburg [11] analyzed the effect of the characteristic length on the numerical accuracy for forward problems. The results showed that six constant or linear elements per wavelength are sufficient to obtain a solution of about error of 10~15%. The quadratic elements seem to provide higher efficiency rates than constant or linear elements.

For BEM-based method, the ill-posed nature may amplify the errors in the inverse procedures [7]. Therefore the requirements for the numbers of elements per wavelength may be more restrictive. The other factors will also affect the reconstruction accuracy. Finding the relationship between the accuracy and the relevant factors, it will be helpful for setting up meshed model and measurement, and selecting appropriate regularization methods and other parameters.

Relevant issues, including element shapes, shape functions, different regularization methods, element

* E-mail: yanghannkim@kaist.ac.kr

characteristic length, measuring distance, and numerical integral methods, are readily addressed and investigated. Numerical simulations compare the performance of the triangle and quadrilateral elements, with three types of interpolation polynomials. Based on the comparison of the reconstruction errors, it is estimated that how many elements per wavelength are required to remain to reach a desired error.

2. Basic theory of BEM-Based NAH

Assuming a sound source in the free space, V_s and V_f imply the interior and the exterior volume, respectively, S_s denotes the source boundary. The acoustic pressure with frequency f at any field point can be computed by Helmholtz's integral equation (HIE) as follows:

$$Cp(r,f) = \iint_{S_s} \left(p(r_s,f) \frac{\partial G(r,r_s,f)}{\partial n_s} - j\rho\omega \, v_n(r_s,f) G(r,r_s,f) \right) dS_s \quad (1)$$

where $p(r,f)$ means the complex pressure in the field with the coordinate r, $p(r_s,f)$ and $v_n(r_s,f)$ mean the pressure and the normal velocity on the surface, respectively. $G(r,r_s,f)$ is Green's function in free space with wavenumber $k = 2\pi f/c$, where f and c represent the frequency and the wave speed, respectively. n_s denotes the outward normal direction to the source surface. The coefficient C depends on the boundary smoothness.

In BEM-based NAH, Helmholtz's integral equations for both the exterior and surface domains are combined to lead to the transfer matrices between the acoustical variances in the hologram and on the surface. After applying the boundary element method, the integral equation can be calculated numerically, and the relationship between surface and exterior acoustical variances can be built by matrix equations as equations (2) and (3),

$$\mathbf{A}_{ss}\mathbf{P}_s = \mathbf{B}_{ss}\mathbf{V}_s \quad (2)$$

$$\mathbf{P}_h = \mathbf{C}_{hs}\mathbf{P}_s - \mathbf{D}_{hs}\mathbf{V}_s \quad (3)$$

Then, the transfer matrix functions, which relate the measured pressure and surface pressure, or normal velocity, can be obtained as follows：

$$\mathbf{P}_h = [\mathbf{C}_{hs}\mathbf{A}_{ss}^{-1}\mathbf{B}_{ss} - \mathbf{D}_{hs}]\mathbf{V}_s = \mathbf{T}_v\mathbf{V}_s \quad (4)$$

$$\mathbf{P}_h = [\mathbf{C}_{hs} - \mathbf{D}_{hs}\mathbf{B}_{ss}^{-1}\mathbf{A}_{ss}]\mathbf{P}_s = \mathbf{T}_p\mathbf{P}_s \quad (5)$$

where $\mathbf{P}_h$ is the vector of pressure on the measurement positions, $\mathbf{P}_s$ and $\mathbf{V}_s$ are the vectors of pressure and normal velocity on the nodes in the surface, respectively. $\mathbf{T}_p$ and $\mathbf{T}_v$ are both transfer matrices. Then the surface pressure and velocity can be calculated in an inverse procedure.

Problematic frequencies are encountered in the BEM-based NAH, which will cause non-unique solution. Combined Helmholtz Integral Equation Formulation (CHIEF) and Burton-Miller method are choices for conquer the problematic frequencies [12,13]. Here CHIEF method is adopted in simulations.

Usually, the regularization methods should be employed to alleviate the ill-posed nature in the inverse procedures. Tikhonov regularization method is broadly used with different manners for selecting regularization parameters [6-7, 14]. Generalized Cross Validation (GCV) and L-curve methods are often hired to determine the regularization parameters. The iterative methods are preferable to obtain the solution of a matrix formula when the matrix is so large that it is too time consuming or too memory-demanding to work with the SVD. Williams [7] explained the similar regularization effect between Krylov subspace iterative method and Tikhonov method. In mathematics, the generalized minimal residual method (GMRES) is an iterative method for the numerical solution of a nonsymmetric system of linear equations [15]. The method approximates the solution by the vector in a Krylov subspace with minimal residual. Both Tikhonov regularization and GMRES are adopted to deal with the inverse procedures and their results are compared.

3. Effect of element type and shape function

Boundary elements can be distinguished due to their shape and shape function (or interpolation). Here they are distinguished by their shape, triangular and quadrilateral, or alternatively, by the order of interpolation, constant, linear and quadratic.

Using the shape function, the coordinate can be expressed as follows,

$$X_i(\xi) = \sum_l N_l(\xi) X_l \quad (6)$$

where $X_i(\xi)$ $(i = 1,2,3)$ are the global Cartesian coordinates and $(\xi) = (\xi_1, \xi_2)$ is the local coordinates, $(l = 3,4,6, or\ 8)$, $N_l(\xi)$ is the shape function. In the same way, the pressure and velocity can be determined by equation 6 as long as replacing the X_l by p_l or v_l.

In this section, the influence of the different element types and shape functions will be studied and then suggestions will be made.

3.1. Forward calculation accuracy versus measurement distance

The measurement distance will be researched firstly. A pulsate sphere is employed to test the

accuracy in forwards calculation. Figure 1 presents meshed models with radius of 0.5m by 384 quadrilaterals and 768 triangles, respectively. All of the constant, linear and quadratic shape function will be adopted and compared. The number of elements and nodes are summarized in Table 1. The characteristic length h is nearly equal to 0.1m.

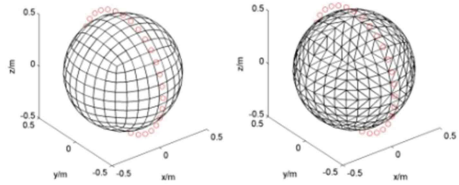

(a) (b)

Figure 1. Meshed model andmeasurement points. (a) 384 quadrilaterals, (b) 768 triangles

Table 1. # of nodes for different shape functions

Elements	Shape function	# of nodes
Quadrilateral (#: 384)	constant	384
	linear	386
	quadratic	1154
Triangle (#: 768)	constant	768
	linear	386
	quadratic	1538

The theoretical pressure and velocity can be calculated by equations 7 and 8, respectively.

$$P = \frac{A}{r} e^{-kr} \tag{7}$$

$$V = \frac{A}{r\rho c} \frac{1 + ikr}{ikr} e^{-kr} \tag{8}$$

where A is a constant, r is the distance from the center of sphere, k is wavenumber, ρ is the medium density and c is the sound speed.

The pressure on the nodes in a circle, whose center coincides with the sphere origin, will be computed. The error is defined by equation 9 where the suffixes denote that values are computed and theoretical, respectively.

$$error = \frac{|P_{compute} - P_{theory}|_2}{|P_{theory}|_2} \times 100 \tag{9}$$

Measurement distance and characteristic length are considered together. Firstly, the measurement distance varies from 0.01m to 0.10m with a fixed frequency f=510Hz. The results are shown in Figure 2 (a). The constant element shows the worst accuracy, linear performs better and quadratic does the best. The error decreases by the increment of measurement distance. Then the measurement distance is fixed to 0.06m for testing the effect of characteristic length by changing the frequency. Reults in Figure 2(b) show that the higher frequency leads to relatively worse accuracy. It can be found that the measurement distance is the primary factor. The errors are similar between models meshed by triangle and quadrilateral elements with same interpolation, except for the case of constant element with d/h=0.1. It is easy to understand that the double integral points lead to a better accuracy certainly when using constant triangle elements.

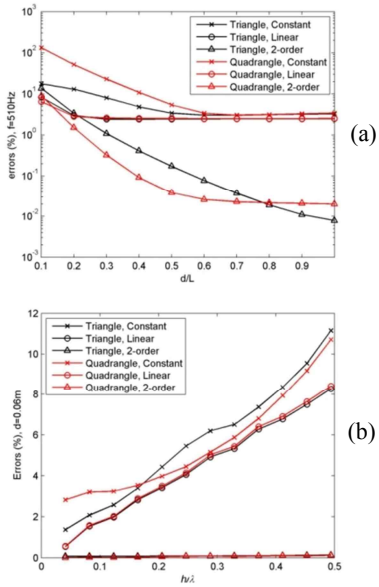

Figure 2: (a) Evolution of the error versus measuring distance for fixed frequency 510Hz; (b) Evolution of the error versus characteristic length for fixed measuring distance 0.06m

For the measurement distance, the errors decrease gradually for constant element until to d/h=0.5, while for linear and quadratic elements until d/h=0.2. For a fixed frequency f = 510Hz, the error approaches to 3% for constant element while d/h>0.5, and 2.5% for linear element while d/h>0.2, and error less than 2% for quadratic element while d/h>0.2. Selecting a fixed distance d=0.06m and changing the frequencies, the error increases for constant and linear elements and it keeps in a small value for quadratic one. When d/h>0.2 and h<λ/4, the forward calculating error is less than 5% for constant elements and 4% for linear elements, and it keeps under 0.5% for quadratic elements.

According to the result above, it prefers to adopt the linear element rather than the constant one, because the higher accuracy requires more evanescent waves existing in near distance. Another reason is that the double nodes in the constant

triangle element model results in large number of measurement points. It reduplicates the working time in practical cases. Therefore, we recommend the characteristic length h to be less than $\lambda/4$ and measurement distance larger than $h/5$ in the linear element models for keeping the forward calculating error under 4%.

Although the quadrilateral element shows the best accuracy, near to 0.1%, it must face the discontinuity feature which leads to large reconstruction error. It is explained in the following section.

3.2. Discontinuity of quadratic element

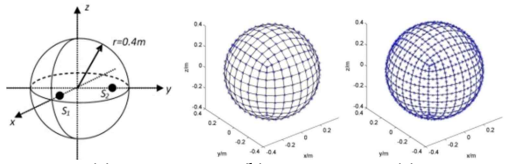

Figure 3. (a) Sound source and meshed model with differrent interpolation, (b) linear and (c) quadratic quadrilateral elements.

A spherical model whose pressure and velocity is excited by two monopole sources is used as the sound source (in Fig. 3). The monopole sources are located at (0, 0.3, 0) and (0.3, 0, 0) with unit of meter, the pressure and velocity excited by a monopole source are calculated by equation 5 and 6 with A=1. The sphere is with radius 0.4m and meshed by 384 linear and quadratic quadrilateral elements, respectively. 1736 measurement points are distributed on a homocentric sphere with radius 0.43m. The frequency is chosen as 100Hz. The reconstructed pressure and velocity on a generatrix in the spherical source surface are used to calculate the errors. They are 5% for pressure and 14% for velocity by the linear elements, and the mean square errors are quite large, more than 25%, for both pressure and velocity by the quadratic elements. The large error is caused by the discontinuity of the quadratic elements.

Williams [7] pointed out that the increasing the resolution by employing the quadratic elements will pay the penalty of reducing the smoothness of the solution. In the procedure of computing $\mathbf{A}_{ss}$, $\mathbf{B}_{ss}$, $\mathbf{C}_{hs}$ and $\mathbf{D}_{hs}$ in equations 2 and 3, the entries of the matrix will be close to 0 which are related to the vertex points of quadratic elements. This unbalance transfers to $\mathbf{T_P}$ and $\mathbf{T_V}$. The details will not be expanded here. Only a simulation is present to explain this discontinuity.

Supposing the singular value decomposition of transfer matrix $[\mathbf{T_V}]_{M\,N}$ in equation 4 is as follows,

$$[\mathbf{T_V}]_{M\,N} = [\mathbf{U}]_{M\,M}[\mathbf{\Sigma}]_{M\,N}[\mathbf{V}]^{H}_{N\,N} \qquad (10)$$

where both $[\mathbf{U}]$ and $[\mathbf{V}]$ are unitary matrices, $[\mathbf{\Sigma}]$ is a diagonal matrix with values $\sigma_1 \geq \cdots \geq \sigma_{N^*} \geq 0$, and $N^* = \mathrm{rank}([\mathbf{T_V}])$. The superscripts H represents Hermitian operator.

$$\mathbf{V}_s = [\mathbf{V}][\mathbf{F}_\alpha][\mathbf{\Sigma}]^{-1}[\mathbf{U}]^{H}\mathbf{P}_h \qquad (11)$$

where $[\mathbf{F}_\alpha]$ is the regularization matrix for alleviate the ill-posed nature. Each column of the $[\mathbf{V}]$ represents an approximation to the acoustic field by basic acoustic waves or mode shapes [7]. The similar performance is for $\mathbf{T_P}$.

The plots of mode shapes in Figure 4 show the discontinuity for the quadratic elements, while the mode shapes perform smooth for linear elements. Therefore, the quadratic elements should be avoided in BEM-based NAH method.

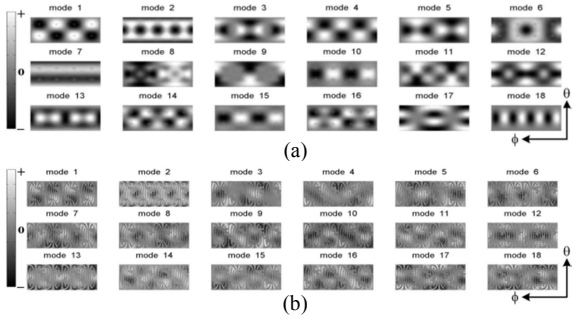

Figure 4. Columns v_1 ,...,v_{18} of [V], which is obtained from the SVD of [**Tv**], f=100 Hz. (a) by linear and (b) quadratic quadrilateral elements.

4. Numerical Experiment

4.1. Sound source model and meshes

The same sound source will be utilized to study the effect of some factors on the reconstruction. The sphere with radius of 0.4m is discretized into 384 quadrilaterals and 768 triangles, and 386 nodes for each. The characteristic length of the element is 0.08m. The frequency varies from 100Hz to 2000Hz. The measurement distance is selected as 0.03m for ensuring the forwards calculation accuracy. There are 488 measurement points distributed evenly on the conformal sphere. Three kinds of regularization methods are adopted simultaneously.

4.2. Errors by characteristic length

Because the reasons explained in section 3, only linear elements are selected to set up the model. Their reconstruction errors versus the ratio of characteristic length on wavelength, h/λ, are plotted in Figure 5.

There is not obvious difference between the errors of both pressure and velocity when using triangle or quadrilateral elements. It means each of them can be employed as per researcher's favor.

The pressure error increases monotonously along with the increment of h/λ. The velocity error decreases firstly when h/λ is in the segment from 0.01 to 1/6 or 1/5, then increases after h/λ exceeds this segment. When h/λ belongs to the segment of [1/10, 1/4], the velocity error is less than 11%. When h is larger than λ/3, both pressure and velocity errors are beyond 16%. Considering to keep both the pressure and velocity errors under an acceptable level as 10%, it is better to set the characteristic length among from 1/10 to 1/4 wavelength.

The different regularization methods also affect the reconstruction errors. As a whole, Tikhonov regularization with GCV or L-curve methods and GMRES lead to similar reconstruction errors, except for velocity errors by triangle elements with small h/λ. Tikhonov method with regularization parameter choosing method of L-curve performs slight better than GMRES while h/λ belongs to [1/10, 1/3]. Tikhonov method with regularization parameter choosing method of GCV performs relatively worse for reconstructing velocity by triangle elements. Especially, when h/λ is in the segment of [1/10, 1/4], there's not obvious difference between errors by GMRES and Tikhonov methods. Therefore, GMRES or Tikhonov method can be chosen freely as per researcher's favor. If Tikhonov method is chosen, it's better to select L-curve method for determining the regularization parameter.

Numerical integral is also a factor for reconstruction accuracy. The Gauss and Hammer numerical integral methods are adopted for quadrilateral and triangle elements, respectively. Usually, more integral points inside the standard element will lead to high resolution [16,17]. For example, using 3×3 Gauss integral points can get the accurate value for 5-order polynomial functions, as well as 4×4 for 7-order and 5×5 for 9-order polynomial functions. But the higher resolution should pay the cost of larger computing time. A test is done to compare the accuracies for different Gauss integral points. The result shown in Figure 6 indicates that only velocity error is reduced slightly for h<λ/5 when the number of Gauss integral points is increased to 25. Hence using 3×3 Gauss integral points is efficient for computing as well as keeping enough resolutions. Correspondingly, to select 7 Hammer integral points is wise for triangle element which is accurate for 5 order polynomial functions.

5. Discussion

The commonly accepted rule of thumb, 6 elements per wavelength, can be extended to a segment that is from 4 to 10 elements per wavelength. In this segment, the velocity error will keep in almost unchangeable level.

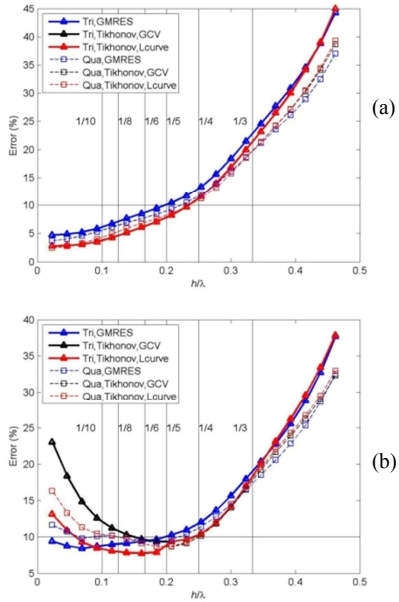

Figure 5. the plots of the reconstruction (a) pressure and (b) velocity accuracy versus h/λ by different element shapes and regularization methods

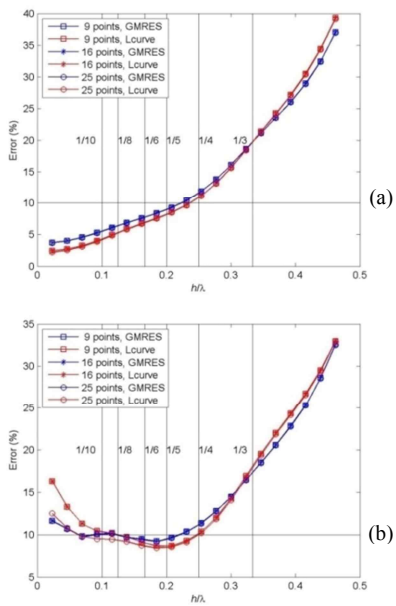

Figure 6. The plots of the reconstruction accuracy versus h/λ under the different number (9, 16 and 25) of gauss integral points, (a) pressure and (b) velocity

According to the analysis for selecting appropriate factors for BEM-based NAH, some items must be discussed firstly. When analyzing the sound field, the

first step is determine the frequency of concern. The second step is to compare the longest and smallest wavelength for cases with a broad band of frequencies, then determine the characteristic length of the element. If the characteristic length of a meshed model cannot satisfy the all frequencies under the rule of $\lambda/10<h<\lambda/4$, for example the expected accuracy is less than 10%, then the model should re-meshed to satisfy the rest frequencies. That means the characteristic length cannot be determined only by the smallest wavelength.

6. Conclusions

The investigated factors include the element type and shape function, measurement distance, characteristic length of element, regularization, and resolution of numerical integral. Their influence on the reconstruction error in BEM-based NAH is studied by numerical simulations. The guide line for determining these factors is summarized seriatim in follows.

Because of the lower resolution of constant element and discontinuity of quadratic element, linear element is suggested for BEM-based NAH. Both triangle and quadrilateral elements can be hired for a designed error level, who perform the similar accuracies.

The measurement distance should be larger than 1/5 of the element characteristic length. To keep the errors of pressure and velocity both fewer than 10%, the meshed model should be limited in from 4 to 10 elements per wavelength. GMRES and Tikhonov method jointly with L-curve method are both suggested for regularization. Numerical integral solution is enough if it's accurate for 5 orders polynomial functions, so that 3×3 Gauss integral points for quadrilaterals and 7 Hammer integral points for triangles are advised.

Acknowledgements

This study is partly supported by National Natural Science Foundation of China (No. 11074170 and No. 11104182) and Brain Korea 21 (BK21) project initiated by Ministry of Education, Science and Technology of Korea.

References

(1) Maynard J.D., Wlliams E.G., Nearfield acoustic holography: I. Theory of generalized holography and the development of NAH. J. Acoust. Soc. Am., 1985, 78(4): 1395-1413

(2) Y.-H. Kim, Can we hear the shape of a noise source?, Plenary Lecture, The 18th International Congress on Acoustic, Kyoto International Conference Hall, Japan, April 4-9, 2004, pp. 3357–3370

(3) Williams E. G., Maynard J. D., Generalized nearfield acoustical holography for cylindrical geometry: theory and experiment. J. Acoust. Soc. Am., 1987, 81(2): 389-407

(4) Bai M. R. S., Application of BEM (boundary element method)-based acoustic holography to radiation analysis of sound sources with arbitrarily shaped geometries. J. Acoust. Soc. Am., 1992, 92 (1): 533-54

(5) Kang S. C., Ih J. G., On the accuracy of nearfield pressure predicted by the acoustic boundary element method. J. Sound Vib., 2000, 233(2): 353-358

(6) Valdivia N., Williams E. G., Krylov subspace iterative methods for boundary element method based near-field acoustic holography. J. Acoust. Soc. Am., 2005, 117(2): 711-724

(7) Valdivia N., Williams E. G., Implicit methods of solution to integral formulations in boundary element method based nearfield acoustic holography. J. Acoust. Soc. Am., 2004, 116(3): 1559-1572

(8) Wang Z., Wu S. F., Helmholtz equation least squares method for reconstructing the acoustic pressure field. J. Acoust. Soc. Am., 1997, 102(4): 2020-2032

(9) Sarkissian A., Method of superposition applied to patch near-field acoustic holography. J. Acoust. Soc. Am. 2005, 118(2): 671-678

(10) Cho Y. T., Bolton J. S., Hald J., Source visualization by using statistically optimized near-field acoustical holography in cylindrical coordinates. J. Acoust. Soc. Am., 2005, 118(4): 2355-2364

(11) Marburg S., Six boundary elements per wavelength is that enough? J. Comput. Acoust., 2002, 10(1): 25-51

(12) Schenk H. A., Improved integral formulation for acoustic radiation problem. J. Acoust. Soc. Am., 1968, 44(1): 41-58

(13) Burton A. J. and Miller G. F., The application of integral equation methods to the numerical solutions of some exterior boundary value problems. Proc. Roy. Soc. London, Series A, 1971, 323: 201-210

(14) Hansen P. C., Regularization tools: A Matlab package for analysis and solution of the discrete ill-posed problems. Version 3.1 for Matlab 6.0, 2001

(15) Saad Y. and Schultz M. H., GMRES: A generalized minimal residual algorithm for solving nonsymmetric linear systems, SIAM J. Sci. Stat. Comput., 1986, 7:856-869

(16) Zienkiewicz O. C., The Finite Element Method in Engineering Science, 2nd edition, McGraw-Hill, London, 1971

(17) Cowper G. R., Gaussian quadrature formulas for triangles. International Journal for Numerical Methods in Engineering, 1973, 7(3): 405-408